

# Wheelchair safety system using fuzzy logic controller to avoid obstruction

Endro Yulianto<sup>1</sup>, Umaimah Mitsalia Ummi Salwa<sup>2</sup>, Triwiyanto<sup>1</sup>, Tri Bowo Indarto<sup>1</sup>

<sup>1</sup>Department of Medical Electronics Technology, Poltekkes Kemenkes Surabaya, Surabaya, Indonesia

<sup>2</sup>Biomedical Engineering Master Degree, Department of Physics, Faculty of Science and Technology, Universitas Airlangga, Surabaya, Indonesia

## Article Info

### Article history:

Received May 6, 2024

Revised Jul 25, 2024

Accepted Aug 6, 2024

### Keywords:

Avoid obstruction

Fuzzy logic controller

Pulse width modulation

Safety wheelchair

Ultrasonic sensor

## ABSTRACT

A wheelchair is the primary means of mobility for individuals unable to walk. This study aimed to develop a safety system for electric wheelchairs to help people with tetraplegia avoid obstructions. The main contribution of this study is the implementation of a sensor with a wider reflection angle and the adjustment of the wheelchair's speed based on the distance to the obstruction, eliminating the need for manual speed selection. The safety system utilizes LV-MaxSonarEZ1 ultrasonic sensors, which function as reflectance distance readers placed on the front, rear, right, and left sides of the wheelchair. The output from the sensors is input into an Arduino, which functions as the controller. The safety system employs adaptive speed control based on distance through a fuzzy logic controller. The wheelchair was tested with obstruction distances of 1, 1.8, 3, and 10 m. The wheelchair could stop at a distance of 34.06 cm for forward movement and 45.16 cm for reverse movement. The results of this study successfully demonstrate the creation of a safety system on a wheelchair using ultrasonic sensors to avoid obstructions and detect areas, with more adaptive speed control based on distance through a fuzzy logic controller.

*This is an open access article under the [CC BY-SA](https://creativecommons.org/licenses/by-sa/4.0/) license.*



## Corresponding Author:

Umaimah Mitsalia Ummi Salwa

Biomedical Engineering Master Degree, Department of Physics, Faculty of Science and Technology,

Universitas Airlangga

Surabaya, Indonesia

Email: umaimah00@gmail.com

## 1. INTRODUCTION

The ease of mobility is one of the most important characteristics that can improve people's quality of life. People with disabilities rely largely on mobility aids to improve their quality of life [1]. The 2015 inter-census population survey (SUPAS) showed that 8.56% of the population experienced functional difficulties, specifically the inability to carry out normal daily activities. The survey also stated that 3.76% of the population had difficulty walking, with 0.32% being residents who fully needed help from others. Most patients with tetraplegia caused by spinal cord injury (SCI) have limitations in using limb functions, which leads to dependence on activities of daily living [2]–[4]. A wheelchair is one of the most important mobility aids for persons with disabilities [1], [5]–[7]. Wheelchairs are designed to allow users to move independently and comfortably. They can be controlled using various systems, such as voice recognition [8]–[10], joystick control [11]–[14], electroencephalograph (EEG) signal [15], [16] or electromyography (EMG) signals [17]–[22]. Safety features, such as obstruction detection, are crucial for maintaining a safe distance from obstructions [23], [24]. Effective safety control in wheelchairs is challenging if the user relies solely on biological signal control, so proximity sensors must be added [17].

Previous study on wheelchair control using EMG signals from the neck and shoulder muscles succeeded in moving the wheelchair forward, backward, right, and left. However, users have difficulty stopping the wheelchair quickly if there is an obstruction [25]. This necessitates collaboration between control systems and safety systems in wheelchairs. Moreover, this safety system can enhance user security [26], [27]. The quest for an effective safety system has led researchers to test various types of sensors. Each sensor, however, has its limitations [28], [29]. Ultrasonic sensors are the most widely used for detecting obstructions [30]. The Parallax PING sensor can measure distances, but its limited detection range requires an increased number of sensors [31]. The HC-SR04 sensor is widely available and commonly used for wheelchair safety, but its reflection angle is only  $\pm 15^\circ$ , which widens the blind spot against obstructions [28]. Ultrasonic sensors are usually installed at the front or back of the wheelchair to detect and stop obstructions at a predetermined distance. In Ruzaij and Poonguzhali's research [32], the set distance was 1 m, but the average wheelchair stopped at 0.4 m from an obstruction due to inertia force. Thus, it is necessary to regulate motor speed when the sensor detects an obstruction to ensure the wheelchair stops completely at the set distance. In Debnath *et al.* research [33], wheelchair speed was controlled using Android-based pulse width modulation (PWM), resulting in more linear and comfortable speed changes for the user. However, user-controlled speed adjustment via Android made the wheelchair less responsive to the environment and required higher user precision. Furthermore, Sankardoss and Geethanjali [34] compared speed control between proportional-integral-derivative (PID) and fuzzy logic controllers. The study found that PID control produced a significant overshoot when there was a change in speed, either accelerating or decelerating. Adding a fuzzy logic controller for speed regulation made the wheelchair movement smoother and safer when there was a control system error or user command error, helping avoid collisions or obstructions [35].

Based on the problems and references identified above, it can be concluded that the previously used ultrasonic sensor in wheelchairs has a limitation of a narrow  $15^\circ$  reading angle, resulting in a wider blind spot. Another issue is that people with disabilities still find it difficult to use Android-based PWM speed controllers. This research aims to design an adaptive safety system for a wheelchair by addressing these problems. The solution involves replacing the sensor with one that has a wider range, specifically the LV-MaxSonarEZ1 sensor, which provides a detection and distance range from 0 to 254 inches and transmits light with a beam width of  $33^\circ$  [36]. Additionally, to address the speed regulation issue, this study proposes an adaptive speed control system that automatically adjusts the wheelchair's speed based on the distance to the obstruction. A fuzzy logic controller system will be used to regulate the motor speed based on PWM.

## 2. METHOD

### 2.1. Experimental setup

The study employed an ultrasonic sensor (LV-MaxSonarEZ1) that detected objects from 0 inches to 254 inches (6.45 m) and supplied sonar range information with a resolution of 1 inch. The available interface output forms include pulse width output, analog voltage output, and serial output [37]. This sensor transmitted a beam with a width of  $33^\circ$  [36]. The movement of the wheelchair is controlled using EMG signal detection and four LV-MaxSonarEZ1 ultrasonic sensors to detect impact distance and adjust speed using fuzzy logic control. As shown in Figure 1, the four sensors are located at the front, rear, right, and left of the wheelchair.

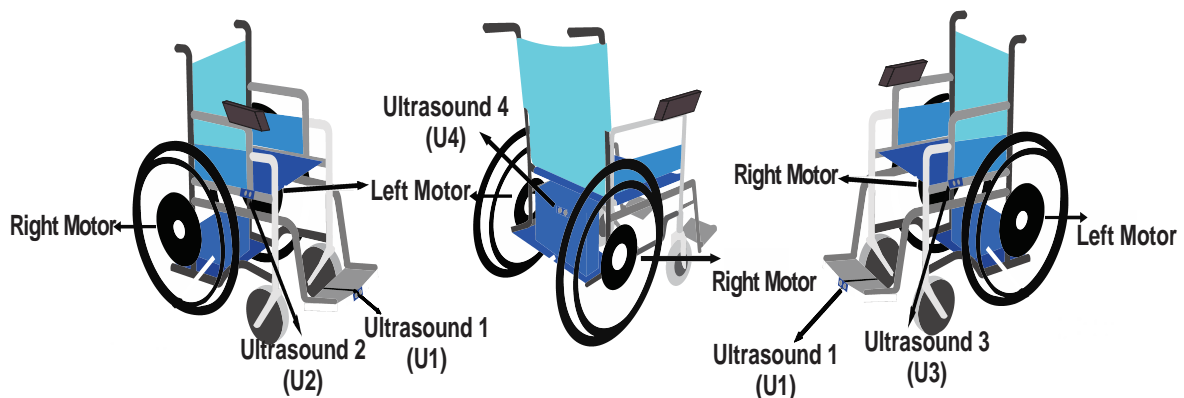


Figure 1. Wheelchair with 4 ultrasonic sensors LV-MaxSonarEZ1

Figure 2 explains how the system works. The system starts from the input block, which receives commands from the EMG signals and the LV-MaxSonarEZ1 ultrasonic sensors. EMG signals serve as inputs for wheelchair movement commands such as forward, backward, right, and left. These inputs are handled by an Arduino Nano. Fuzzy logic control takes the distance data from the ultrasonic sensors to generate PWM values, which are classified as rapid, medium, slow, and stop. The resulting speeds are then connected to the speed control circuit of the right and left motors, respectively [38].

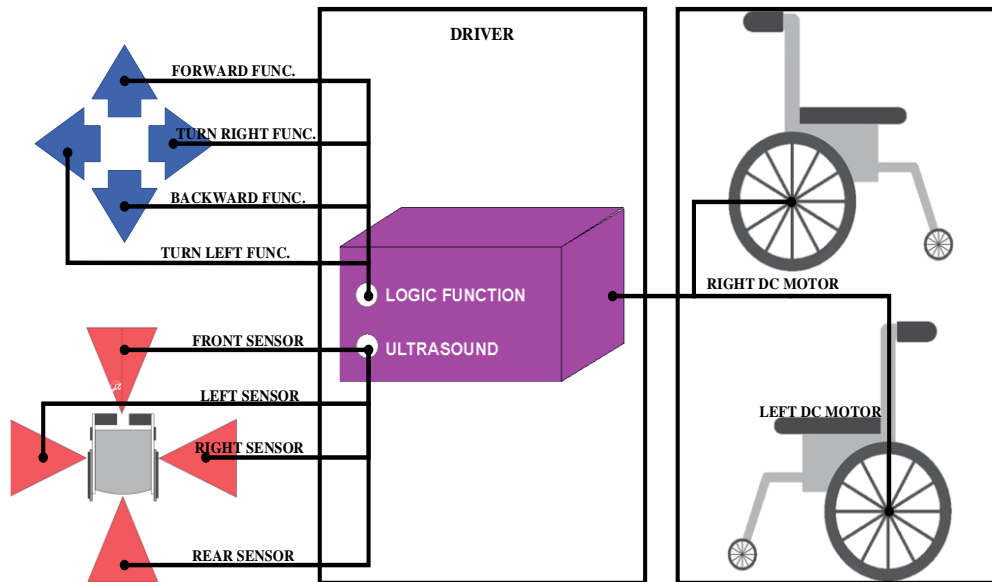


Figure 2. Wheelchair block diagram

The system has two areas: free and corridor. The corridor includes two modes: following the right wall and following the left wall. Figure 3 depicts how the wheelchair uses ultrasonic sensors to choose a region. Obstruction measurements are performed by sensors U2 (left-side sensor) and U3 (right-side sensor).

Figure 3(a) depicts the left wall-following mode. When U2 (left-side sensor) identifies a short distance to an impediment, the wheelchair moves forward while remaining safe from the left wall. If U3 (the right-side sensor) detects an obstruction at a short distance, the wheelchair advances forward while remaining safe from the right wall, as shown in Figure 3(b). Figure 3(c) shows that if both U2 and U3 identify short distances to barriers, the wheelchair slows down and moves slowly. If both sensors detect very close obstructions, the wheelchair will come to a complete stop.

If neither of these conditions are met, or if both U2 and U3 detect long distances between barriers, the wheelchair enters free mode. In free mode, the ultrasonic sensors detect the obstruction distance and set the motor's PWM value. The distance data obtained from the sensors as the wheelchair goes forward and backward are used as inputs for the fuzzy control. These inputs are then processed to control the motor's PWM.

## 2.2. Pulse width modulation

Pulse width modulation (PWM), or pulse width modulation, is a technique for regulating the pulse width to create the desired output voltage. Originally used in telecommunications, it was later applied in power electronics. The basic principle involves a DC-link voltage,  $V_{dc}$ . The  $V_x$  phase output voltage in Figure 4 alternates between half the positive and negative DC-link voltages by comparing the reference voltages  $V_{ref}$  and the carrier during each switching cycle  $T_s$ .

PWM will form. When the  $V_{ref}$  is greater than the carrier, the up switch in the phase is triggered and the down switch is deactivated. The time  $T_0$  for the negative voltage ( $-V_{dc}/2$ ) satisfies the equation  $T_0/T_s = (V_{dc}/2 - V_{ref})/V_{dc}$ . In (1) shows that the average voltage  $V_x$  in one switching cycle  $T_s$  is equal to  $V_{ref}$  [39].

$$V_x = \frac{1}{T_s} \times \left[ (T_s - T_0) \times \frac{V_{dc}}{2} + (-\frac{V_{dc}}{2}) \right] = V_{ref} \tag{1}$$

**2.3. Fuzzy logic controller**

Fuzzy logic has a degree of membership between 0 and 1, as opposed to classical Boolean logic, which only has 0 and 1 values [40]. Fuzzy logic processes include fuzzification, rule base, inference, and defuzzification, as illustrated in Figure 5. This method makes systems more flexible and adaptive, allowing for better handling of uncertainty and imprecision in complex contexts.

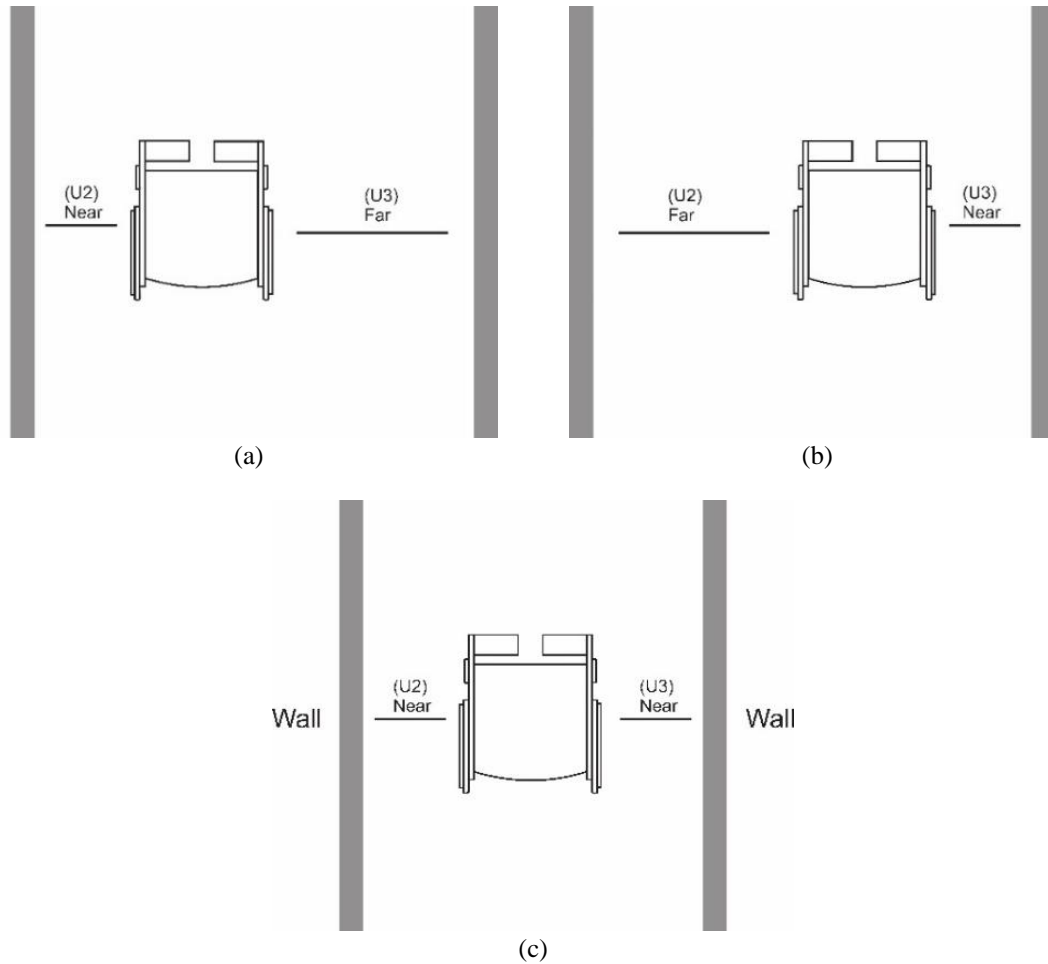


Figure 3. Shows how a side ultrasonic sensor maps (a) the left wall, (b) the right wall, and (c) the two-side obstruction

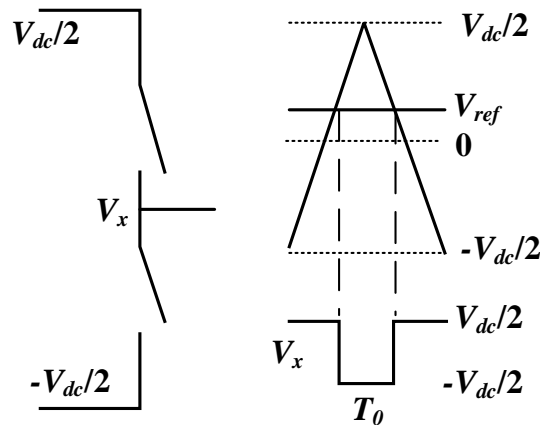


Figure 4. Pulse width modulation

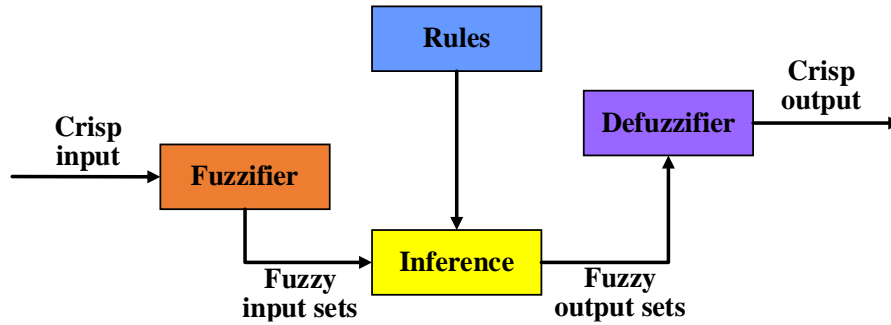


Figure 5. Fuzzy logic control system architecture

- Fuzzification is the process of turning input values to fuzzy values (linguistic variables). While other curves are utilized in the literature, the Gaussian, triangular, and trapezoidal membership functions are the most typically employed in fuzzification processes. In [40], the membership function is calculated using (2):

$$f(x, a, b, c) = \begin{cases} 0, & x \leq a \\ \frac{x-a}{b-a}, & a \leq x \leq b \\ \frac{c-x}{c-b}, & b \leq x \leq c \\ 0, & c \leq x \end{cases} \quad (2)$$

where  $f(x, a, b, c)$  is the degree of membership,  $x$  is the value of the variable, successively  $a, b, c$  is the initial, middle, and end values of the variable as shown in Figure 6.

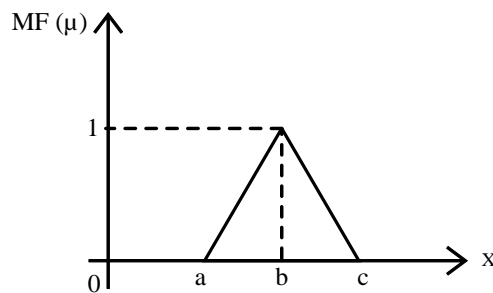


Figure 6. Fuzzy set of triangles

- The rule base contains the decision-making rules. Each rule has two major components: an antecedent block (between “If” and “Then”) and a consequent block (after “Then”).
- Inference determines the fuzzy judgments made throughout the rule base process, which results in a fuzzy collection of decisions. Logical operators, such “AND,” “OR,” and “NOT,” specify how fuzzy variables are joined.
- Defuzzification is the reverse of the fuzzification process; it converts the fuzzy output into crisp values to be applied to the system [41].

This study employs the Takagi-Sugeno-Kang (TSK) approach, which is simpler to implement in programming languages due to its singleton set on the output variable. As a result, the defuzzification procedure is simplified. Furthermore, the TSK method offers a more efficient and computationally effective solution for real-time applications and control systems. In [40], the output equation of the TSK method is:

$$Z_{out} = \frac{\sum_{i=1}^n w_i z_i}{\sum_{i=1}^n w_i} \quad (3)$$

where  $Z_{out}$  is the crisp output value,  $w_i$  is the degree of membership of the  $i$ -th value and  $z_i$  is the output value of the  $i$ -th variable.

## 2.4. Technical application of fuzzy logic

This method describes the technique utilized. Figure 7(a) shows the fuzzy logic mechanism while the wheelchair is in a free region. The distance between the wheelchair and an obstruction is divided into four segments: 9 m, 3 m, 1.8 m, and 1 m. The results of the sensor readings serve as the input for fuzzy logic control, which then produces an output as PWM for the motor to prevent collisions.

Figures 7(b) and 7(c) show the mechanisms for the right and left sides of the corridor. For the corridor area, the system employs the error value calculated from the difference between the distance read and the predetermined (safe) distance. The data collection in this experiment began by establishing an initial distance between the wheelchair and the wall. The sensor then adjusts the wheelchair's position to maintain the specified distance from the wall.

## 2.5. Fuzzification

In this process, the crisp value (output from the sensor) is converted into a membership level of fuzzy set linguistic terms. The membership function for distance in Figure 7(a) is shown in Figure 8, and its error in Figure 7(b) and Figure 7(c) is shown in Figure 9. This conversion involves transforming the exact numerical value of the sensor into degrees membership corresponding to a linguistic term in a fuzzy set. The membership function is a curve that transfers each point in the input space to a membership value ranging from 0 to 1, indicating how much of the input belongs to the fuzzy set. The membership function for distance illustrated shows how sharp distance values are categorized into terms such as “*very near (vn)*,” “*near (nr)*,” “*far (fr)*,” and “*very far (vfr)*.” Similarly, membership functions for errors, explain how various levels of errors are classified into terms such as “*negative big (nb)*,” “*negative medium (nm)*,” “*negative small (ns)*,” “*zero (ze)*,” “*positive small (ps)*,” “*positive medium (pm)*,” or “*positive big (pb)*.”

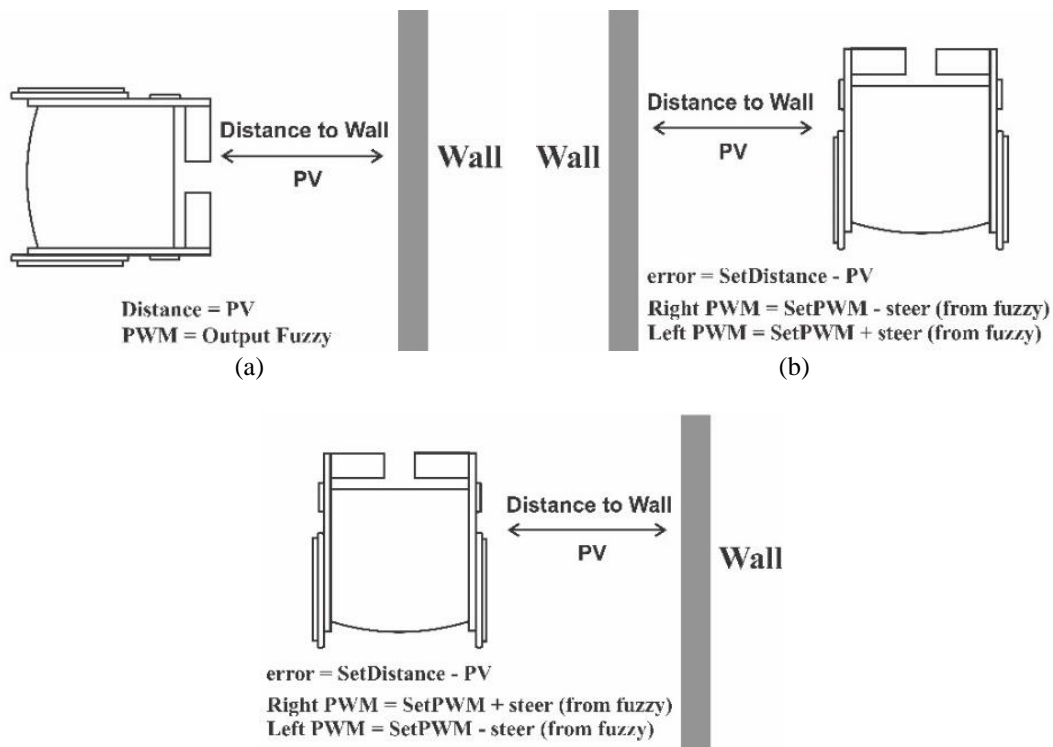


Figure 7. Technical movements for (a) wheelchair mobility forward or backward in a free area, (b) left wall following mode, and (c) right wall following mode

## 2.6. Rule base interference

In this study, the researcher proposed a basis of inference rules for free areas and hallway areas, as shown in Table 1 and Table 2. For free areas, four rules were used. In Table 1, if the distance is very near (*vn*), then PWM is very slow (*vs*). If the distance is near (*nr*), then PWM is slow (*sl*). If the distance is far (*fr*), then PWM is fast (*fs*). If the distance is very far (*vfr*), then PWM is very fast (*vf*). For the hallway area, a wall-following program was used with a specified distance and a total of seven rules. In Table 2, if the

error value is smaller (more negative or NB), then the steering value is also smaller ( $O_{NB}$ ). If the error value is zero (ze), then the steering value is also zero ( $O_{ZE}$ ). If the error value is larger (more positive or pb), then the steering value is also larger ( $O_{PB}$ ).

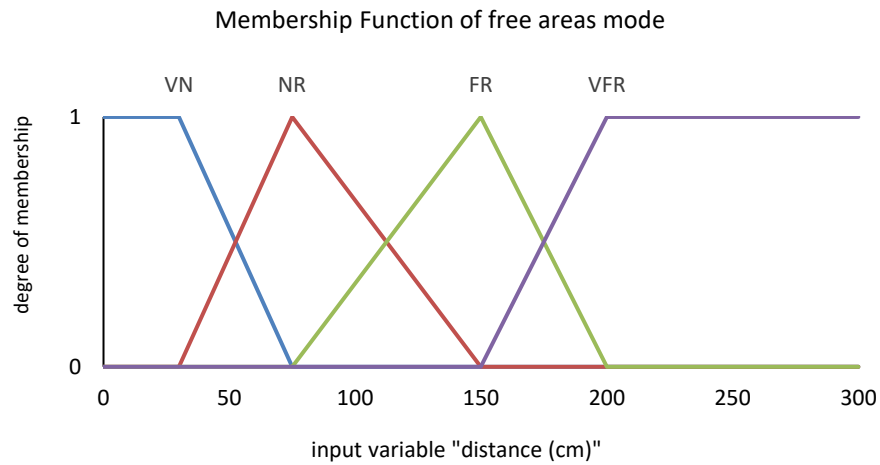


Figure 8. Membership fuzzification for forward and reverse command-free areas

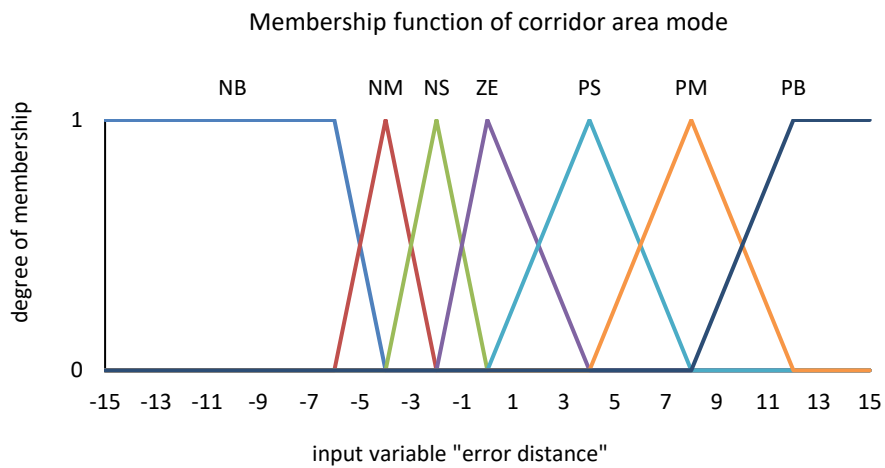


Figure 9. Membership function for corridor areas

Table 1. Rule base for the free area

Input	Output
<i>if (DISTANCE is vn)</i>	<i>then (PWM is vs)</i>
<i>if (DISTANCE is nr)</i>	<i>then (PWM is sl)</i>
<i>if (DISTANCE is fr)</i>	<i>then (PWM is fs)</i>
<i>if (DISTANCE is vfr)</i>	<i>then (PWM is vf)</i>

Table 2. Rule base for wall following behavior

Input	Output
<i>if (ERROR is nb)</i>	<i>then (STEER is O_NB)</i>
<i>if (ERROR is nm)</i>	<i>then (STEER is O_NM)</i>
<i>if (ERROR is ns)</i>	<i>then (STEER is O_NS)</i>
<i>if (ERROR is ze)</i>	<i>then (STEER is O_ZE)</i>
<i>if (ERROR is ps)</i>	<i>then (STEER is O_PS)</i>
<i>if (ERROR is pm)</i>	<i>then (STEER is O_PM)</i>
<i>if (ERROR is pb)</i>	<i>then (STEER is O_PB)</i>

## 2.7. Defuzzification

This study employed fuzzy Sugeno, therefore the membership function took the form of a rod. The output membership function of the PWM setting in the free area following the wall is shown in Figure 10. Meanwhile, the output membership displacement of the PWM setting in the free area following the wall is shown in Figure 11.

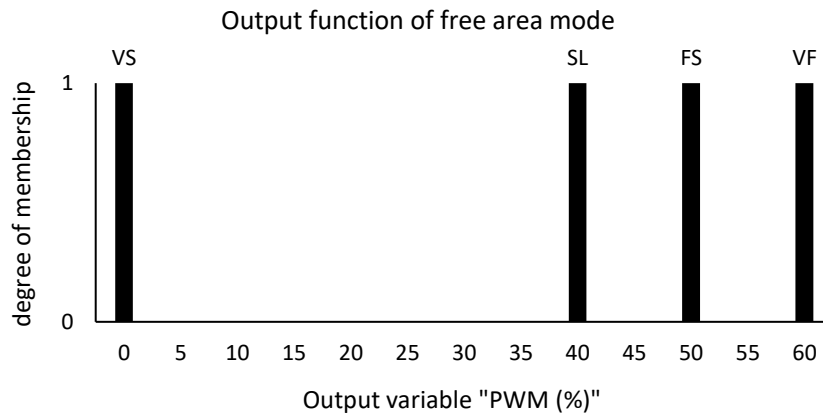


Figure 10. Membership function for speed defuzzification output from free areas

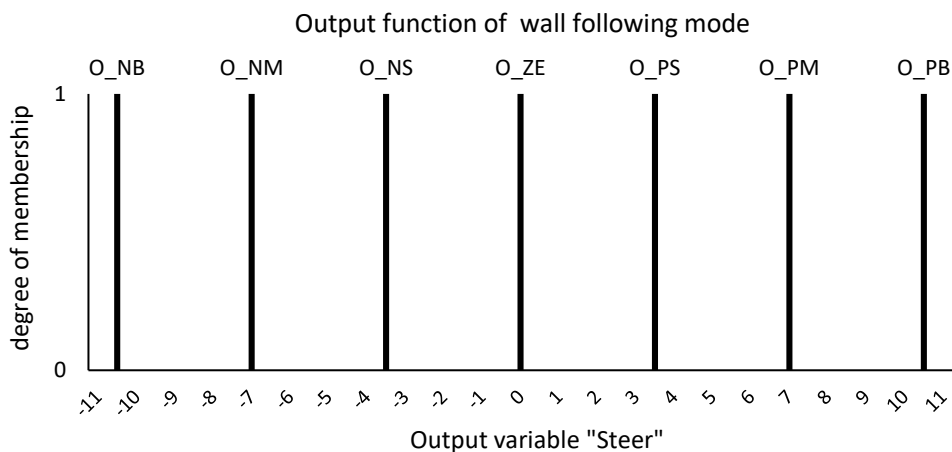


Figure 11. Membership function for steering defuzzification output from corridor areas

## 3. RESULTS AND DISCUSSION

### 3.1. Decrease in PWM value

According to Figure 12, when the wheelchair approaches an obstruction, the initial drop distance is 200 cm from the sensor to the barrier. This also occurs as the wheelchair moves backwards. At the initial drop from 200-70 cm, the drop process involves a large decrease of up to 9% in PWM. In the subsequent decline, there is a sharp drop. When the wheelchair moves forward, the PWM decrease reaches 4.3%. Meanwhile, when the wheelchair moves backward, the decrease in PWM reaches 4.7%. This causes the motor to no longer be strong enough to move the wheelchair.

In prior experiments, wheelchairs with PWM control were more linear and comfortable with percentages of 40%, 60%, 80%, and 100%. However, the right and left motors received PWM values from Android commands [33]. This method allows the wheelchair to move at varied rates depending on the distance to the impediment, which improves user safety. Furthermore, for distances higher than 200 cm, the wheelchair moves swiftly and gradually decreases speed. Moving forward, the average distance between the wheelchair and the impediment was 34.06 cm. When traveling rearward, the wheelchair stops at an average distance of 45.16 cm.



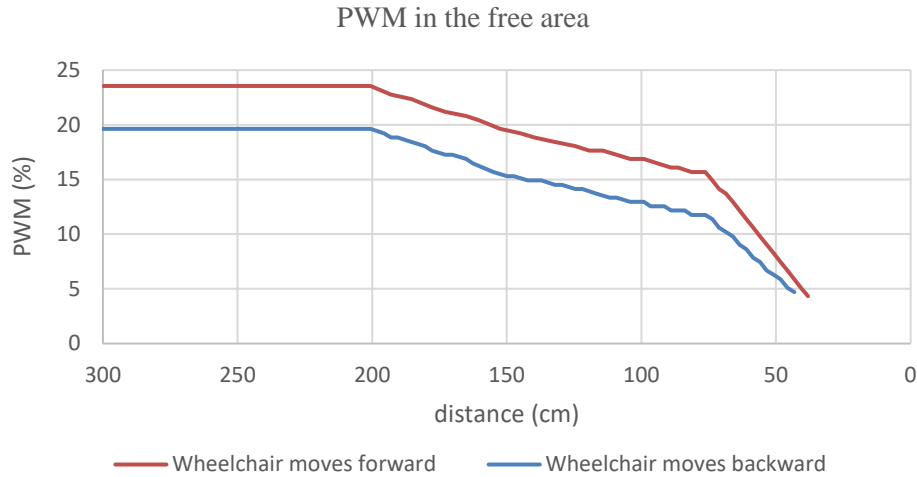


Figure 12. PWM graph as the wheelchair moves forward and backward in the free area toward the obstruction

### 3.2. Corridor area

Figure 13 shows that both studies started at a distance of 40 cm. Both wheelchairs simultaneously moved away when they detected the distance. Subsequently, the sensor adjusted the wheelchair's position to maintain the set distance from the wall. In the right-following mode, the farthest distance between the wheelchair and the right wall was 68 cm, while the closest distance was 28 cm. In this case, there was a spike in the data obtained by the sensor, likely due to interference from other sensors. Meanwhile, in the left-following mode, the farthest gap between the wheelchair and the left wall was 56 cm, and the closest was 28 cm.

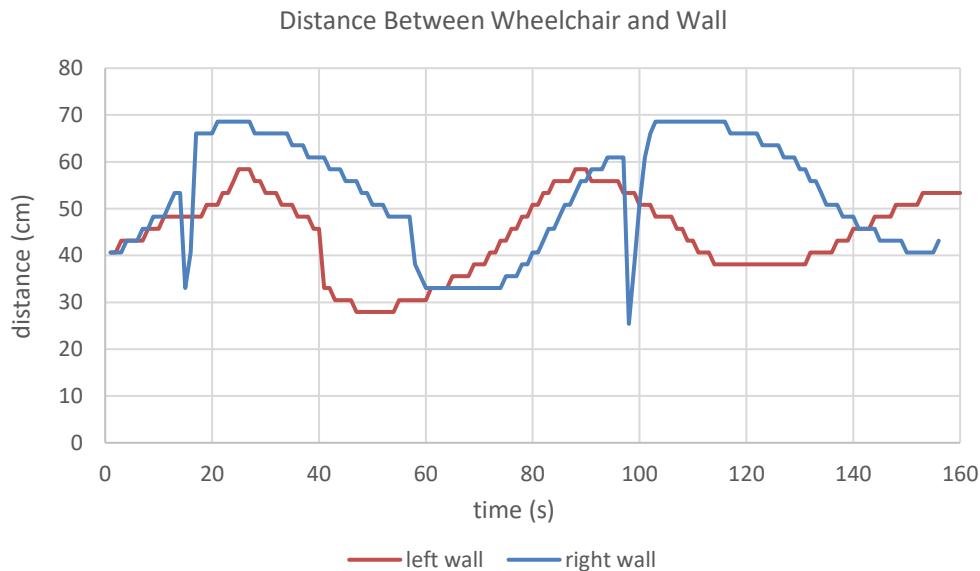


Figure 13. The graphic depicts the distance between the wheelchair and the wall in the corridor area

In the actual setup, the right and left motor PWM configurations were adjusted to enable the wheelchair to track a straight line. However, it encountered erratic movements. The ultrasonic sensor readings were translated into PWM values in the corridor region to allow the wheelchair to move straight along the right or left wall; nonetheless, the wheelchair still displayed winding movements [42]. As shown in Figure 13, The ultrasonic sensor data indicated that the distance between the wheelchair and the wall during movement ranged from 28 to 68 cm, and the wheelchair's movement was still too winding.

### 3.3. Sensor reading area

An experiment was conducted to determine the width of the sensor coverage area using a 5 cm wide brick with a flat surface. The sensor can detect obstructions up to  $\pm 30^\circ$  at a distance of 100 cm. Figure 14 illustrates how the shape and surface area of the obstacle influenced the sensor response.

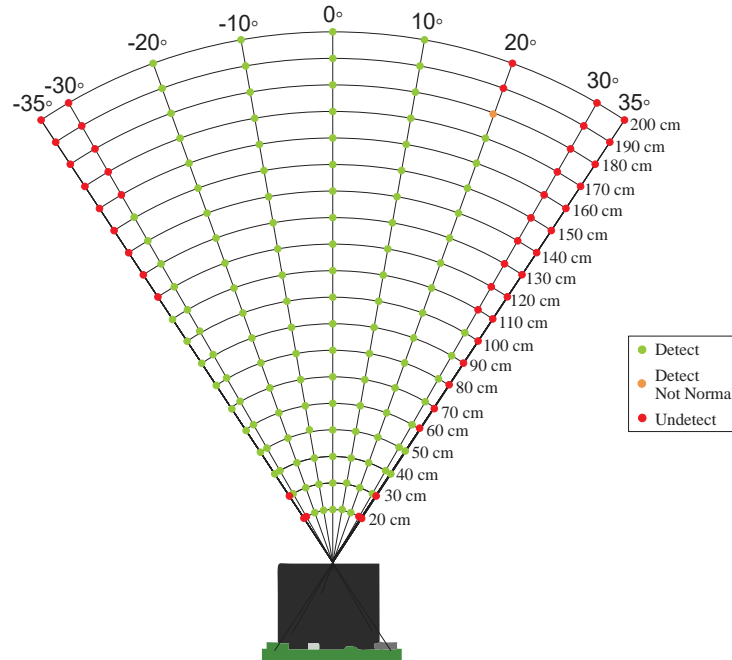


Figure 14. LV-MaxSonarEZ1 reading area mapping

## 4. CONCLUSION

The goal of this study was to develop a wheelchair with EMG control and an adaptive safety system employing fuzzy logic control. The LV-MaxSonar EZ1 ultrasonic sensor can detect obstructions up to  $\pm 30^\circ$ , providing a broader sensor range than the HC-SR04 sensor. The sensor response is affected by the form and surface area of the impediment being read. Furthermore, the results of this research show that the wheelchair safety control design can reduce speed linearly when an obstruction is detected, converting linguistic input from distance readings into PWM for motor output using a fuzzy logic controller. The wheelchair starts to reduce its speed at a distance of 2 m. The wheelchair can operate a safety riding system in both free areas and hallways. It can stop at an average distance of 34.06 cm when moving forward and at an average distance of 45.16 cm when moving backward. To acquire the best results, it is vital to determine the precise location of the sensor and consider the movement of the wheels to avoid altering sensor readings when the wheelchair is moving. Excessive use of multisensory systems needs to be minimized to prevent sensor data loss, which can affect the fuzzy process. Therefore, a self-test is needed on the wheelchair to ensure that all sensors are functioning properly. The research results can be implemented as a safety system solution for wheelchairs for tetraplegic sufferers to help support their daily lives.

## REFERENCES




- [1] F. Utaminigrum *et al.*, "Development of computer vision based obstacle detection and human tracking on smart wheelchair for disabled patient," in *5th International Symposium on Computational and Business Intelligence*, Aug. 2017, pp. 1–5, doi: 10.1109/ISCBI.2017.8053533.
- [2] J. H. Jung *et al.*, "Effects of combined upper limb robotic therapy in patients with tetraplegic spinal cord injury," *Annals of Rehabilitation Medicine*, vol. 43, no. 4, pp. 445–457, 2019, doi: 10.5535/arm.2019.43.4.445.
- [3] W. Tigra *et al.*, "A novel EMG interface for individuals with tetraplegia to pilot robot hand grasping," *IEEE Transactions on Neural Systems and Rehabilitation Engineering*, vol. 26, no. 2, pp. 291–298, 2018, doi: 10.1109/TNSRE.2016.2609478.
- [4] M. A. Kader, M. E. Alam, N. Jahan, M. A. B. Bhuiyan, M. S. Alam, and Z. Sultana, "Design and implementation of a head motion-controlled semi-autonomous wheelchair for quadriplegic patients based on 3-axis accelerometer," in *2019 22nd International Conference on Computer and Information Technology (ICCIT)*, Dec. 2019, pp. 1–6, doi: 10.1109/ICCIT48885.2019.9038512.
- [5] E. Kim, "Wheelchair navigation system for disabled and elderly people," *Sensors*, vol. 16, no. 11, Oct. 2016, doi: 10.3390/s16111806.

- [6] M. Callejas-Cuervo, A. X. González-Cely, and T. Bastos-Filho, "Design and implementation of a position, speed and orientation fuzzy controller using a motion capture system to operate a wheelchair prototype," *Sensors*, vol. 21, no. 13, 2021, doi: 10.3390/s21134344.
- [7] S. U. Upase, "Speech recognition based robotic system of wheelchair for disable people," *2016 International Conference on Communication and Electronics Systems (ICCES)*, Coimbatore, India, 2016, pp. 1-5, doi: 10.1109/CESYS.2016.7889851.
- [8] M. M. Abdulghani, K. M. Al-Aubidy, M. M. Ali, and Q. J. Hamarsheh, "Wheelchair neuro fuzzy control and tracking system based on voice recognition," *Sensors*, vol. 20, no. 10, May 2020, doi: 10.3390/s20102872.
- [9] L. Chen, S. Wang, H. Hu, D. Gu, and I. Dukes, "Voice-directed autonomous navigation of a smart-wheelchair," in *Smart Wheelchairs and Brain-computer Interfaces: Mobile Assistive Technologies*, Second Edi., Elsevier, 2018, pp. 405–424.
- [10] A. Ruíz-Serrano, R. Posada-Gómez, A. M. Sibaja, G. A. Rodríguez, B. E. Gonzalez-Sanchez, and O. O. Sandoval-Gonzalez, "Development of a dual control system applied to a smart wheelchair, using magnetic and speech control," *Procedia Technology*, vol. 7, pp. 158–165, 2013, doi: 10.1016/j.protcy.2013.04.020.
- [11] M. Shibata, C. Zhang, T. Ishimatsu, M. Tanaka, and J. Palomino, "Improvement of a joystick controller for electric wheelchair user," *Modern Mechanical Engineering*, vol. 5, no. 4, pp. 132–138, 2015, doi: 10.4236/mme.2015.54013.
- [12] Y. Rabhi, M. Mrabet, F. Fnaiech, and P. Gorce, "Intelligent joystick for controlling power wheelchair navigation," in *2013 3rd International Conference on Systems and Control*, 2013, pp. 1020–1025, doi: 10.1109/ICoSC.2013.6750981.
- [13] H. D. Shin *et al.*, "Customized power wheelchair joysticks made by three-dimensional printing technology: A pilot study on the environmental adaptation effects for severe quadriplegia," *International Journal of Environmental Research and Public Health*, vol. 18, no. 14, 2021, doi: 10.3390/ijerph18147464.
- [14] J. H. Choi, Y. Chung, and S. Oh, "Motion control of joystick interfaced electric wheelchair for improvement of safety and riding comfort," *Mechatronics*, vol. 59, pp. 104–114, 2019, doi: 10.1016/j.mechatronics.2019.03.005.
- [15] H. P. C. Anjana, V. R. P. Rao, M. S. A. bin M. Azizi, W. J. Tee, R. K. Murugesan, and M. D. Hamzah, "A proposed web based real time brain computer interface (BCI) system for usability testing," *International journal of online and biomedical engineering*, vol. 15, no. 8, pp. 108–119, 2019, doi: 10.3991/ijoe.v15i08.10406.
- [16] J. Katona and A. Kovari, "EEG-based computer control interface for brain-machine interaction," *International Journal of Online Engineering*, vol. 11, no. 6, pp. 43–48, 2015, doi: 10.3991/ijoe.v11i6.5119.
- [17] H. Tamura, T. Murata, Y. Yamashita, K. Tanno, and Y. Fuse, "Development of the electric wheelchair hands-free semi-automatic control system using the surface-electromyogram of facial muscles," *Artificial Life and Robotics*, vol. 17, no. 2, pp. 300–305, Dec. 2012, doi: 10.1007/s10015-012-0060-2.
- [18] G. Lee, K. Kim, and J. Kim, "Development of hands-free wheelchair device based on head movement and bio-signal for quadriplegic patients," *International Journal of Precision Engineering and Manufacturing*, vol. 17, no. 3, pp. 363–369, 2016, doi: 10.1007/s12541-016-0045-5.
- [19] G. Jang and Y. Choi, "EMG-based continuous control method for electric wheelchair," in *IEEE International Conference on Intelligent Robots and Systems*, 2014, no. Iros, pp. 3549–3554, doi: 10.1109/IROS.2014.6943058.
- [20] Z. Alibhai, T. Burreson, M. Stiller, I. Ahmad, M. Huber, and A. Clark, "A human-computer interface for smart wheelchair control using forearm EMG signals," in *Proceedings - 2020 3rd International Conference on Data Intelligence and Security, ICDIS 2020*, 2020, pp. 34–39, doi: 10.1109/ICDIS50059.2020.00011.
- [21] E. Yulianto, T. B. Indrato., B. TMN, and Suharyati, "Wheelchair for quadriplegic patient with electromyography signal control wireless," *International journal of online and biomedical engineering*, vol. 16, no. 12, pp. 94–115, 2020, doi: 10.3991/ijoe.v16i12.15721.
- [22] A. S. Kundu, O. Mazumder, P. K. Lenka, and S. Bhaumik, "Hand gesture recognition based omnidirectional wheelchair control using IMU and EMG sensors," *Journal of Intelligent and Robotic Systems: Theory and Applications*, vol. 91, no. 3–4, pp. 529–541, 2018, doi: 10.1007/s10846-017-0725-0.
- [23] F. Leishman, O. Horn, and G. Bourhis, "Smart wheelchair control through a deictic approach," *Robotics and Autonomous Systems*, vol. 58, no. 10, pp. 1149–1158, 2010, doi: 10.1016/j.robot.2010.06.007.
- [24] M. Njah and M. Jallouli, "Wheelchair obstacle avoidance based on fuzzy controller and ultrasonic sensors," in *International Conference on Computer Applications Technology*, Jan. 2013, pp. 1–5, doi: 10.1109/ICCAT.2013.6522062.
- [25] E. Yulianto, T. B. Indrato, and S. Suharyati, "The design of electrical wheelchairs with electromyography signal controller for people with paralysis," *Electrical and Electronic Engineering*, vol. 8, no. 1, pp. 1–9, 2018, doi: 10.5923/j.eee.20180801.01.
- [26] T. Masuzawa, K. Tanaka, and S. Minami, "Development of a safety driving system for electric wheelchair," *Journal of Asian Electric Vehicles*, vol. 7, no. 2, pp. 1325–1332, 2009, doi: 10.4130/jaev.7.1325.
- [27] D. A. Sanders, "Using self-reliance factors to decide how to share control between human powered wheelchair drivers and ultrasonic sensors," *IEEE Transactions on Neural Systems and Rehabilitation Engineering*, vol. 25, no. 8, pp. 1221–1229, Aug. 2017, doi: 10.1109/TNSRE.2016.2620988.
- [28] A. Ruíz-Serrano, M. C. Reyes-Fernández, R. Posada-Gómez, A. Martínez-Sibaja, and A. A. Aguilar-Lasserre, "Obstacle avoidance embedded system for a smart wheelchair with a multimodal navigation interface," in *2014 11th International Conference on Electrical Engineering, Computing Science and Automatic Control, CCE 2014*, Sep. 2014, pp. 1–6, doi: 10.1109/ICEEE.2014.6978290.
- [29] S. Desai, S. S. Mantha, and V. M. Phalle, "Advances in smart wheelchair technology," *2017 International Conference on Nascent Technologies in Engineering (ICNTE)*, Vashi, India, 2017, pp. 1-7, doi: 10.1109/ICNTE.2017.7947914.
- [30] J. Pu, Y. Jiang, X. Xie, X. Chen, M. Liu, and S. Xu, "Low cost sensor network for obstacle avoidance in share-controlled smart wheelchairs under daily scenarios," *Microelectronics Reliability*, vol. 83, pp. 180–186, 2018, doi: 10.1016/j.microrel.2018.03.003.
- [31] M. Rojas, P. Ponce, and A. Molina, "Novel fuzzy logic controller based on time delay inputs for a conventional electric wheelchair," *Revista Mexicana de Ingeniería Biomedica*, vol. 35, no. 2, pp. 127–144, 2014.
- [32] M. F. Ruzajj and S. Poonguzhali, "Design and implementation of low cost intelligent wheelchair," in *International Conference on Recent Trends in Information Technology*, 2012, pp. 468–471, doi: 10.1109/ICRTIT.2012.6206809.
- [33] T. Debnath, A. F. M. Z. Abadin, and M. A. Hossain, "PWM based Android controlled wheel chair," *International Journal of Computer Science and Information Technology*, vol. 10, no. 2, pp. 57–64, 2018, doi: 10.5121/ijcsit.2018.10205.
- [34] V. Sankardoss and P. Geethanjali, "Design and low-cost implementation of an electric wheelchair control," *IETE Journal of Research*, vol. 67, no. 5, pp. 657–666, 2021, doi: 10.1080/03772063.2019.1565951.
- [35] G. Pires and U. Nunes, "A wheelchair steered through voice commands and assisted by a reactive fuzzy-logic controller," *Journal of Intelligent and Robotic Systems: Theory and Applications*, vol. 34, no. 3, pp. 301–314, 2002, doi: 10.1023/A:1016363605613.
- [36] H. Seydroudbari *et al.*, "Design and implementation of a two-dimensional ultrasonic radar using FPGA," in *Senior Design Fall*, 2018, pp. 1–8.




- [37] MaxBotix, "LV - MaxSonar @- EZ™ Series," *maxbotix.com*, 2015. Accessed: Dec. 30, 2022. [Online], Available: <https://maxbotix.com/pages/lv-maxsonar-ez-datasheet>
- [38] R. G. Klimo, "Electric wheelchair with improved control circuit," U.S. Patent 4,634,941, Jan. 6, 1987.
- [39] D. Jiang, Z. Shen, and Q. Li, *Advanced modulation: with freedom to optimize power electronics converters*. Springer, 2021.
- [40] T. Sutikno, A. C. Subrata, and A. Elkhateb, "Evaluation of fuzzy membership function effects for maximum power point tracking technique of photovoltaic system," *IEEE Access*, vol. 9, pp. 109157–109165, 2021, doi: 10.1109/ACCESS.2021.3102050.
- [41] E. Kayacan and M. A. Khanesar, "Fundamentals of type-1 fuzzy logic theory," *Fuzzy Neural Networks for Real Time Control Applications*, pp. 13–24, 2016, doi: 10.1016/b978-0-12-802687-8.00002-5.
- [42] E. Yulianto *et al.*, "Obstacles and areas detection based on pulse width modulation method for electric wheelchair safety using ultrasound sensors," *Journal of Biomimetics, Biomaterials and Biomedical Engineering*, vol. 50, pp. 73–88, 2021, doi: 10.4028/www.scientific.net/JBBBE.50.73.

## BIOGRAPHIES OF AUTHORS






**Endro Yulianto**    born in Banyubiru, 17 July 1976, Diploma of Academy of Electro Health Department, Indonesia, 1997, Graduate of Nuclear Engineering of Universitas Gadjah Mada, Yogyakarta, Indonesia, 1999, master in Institut Teknologi Sepuluh Nopember Surabaya, Indonesia, 2004, Graduate of Electronics Engineering of Engineering Faculty, Universitas Gadjah Mada, Yogyakarta, Indonesia, 2013. From 2001 until now, he has worked in the medical electronics engineering technology, at Health Polytechnic of Surabaya. He can be contacted at email: endro76@poltekkesdepkes-sby.ac.id.






**Umaimah Mitsalia Umami Salwa**    born in Surabaya in January 2000. After earning her bachelor's degree in the medical electronics engineering technology, at Health Polytechnic of Surabaya in 2022, She continues her academic journey at Airlangga University, where she is currently pursuing his master's studies. She can be contacted at email: umaimah00@gmail.com.



**Triwiyanto**    received the B.S. degree in physics from Airlangga University, Indonesia, M.S. degrees in electronic engineering from the Institut Teknologi Sepuluh Nopember Surabaya, Indonesia in 2004, and the Ph.D. degree in electrical engineering from Gadjah Mada University, Yogyakarta, Indonesia, in 2018. From 1998 to 2004, he was a senior lecturer with the Microcontrollers Laboratory. Since 2005, he has been an assistant professor with the Medical Electronics Technology Department, Health Polytechnic Ministry of Health Surabaya, Indonesia. In 2018, Triwiyanto received the Best Doctoral Student Award from Gadjah Mada University. Additionally, he is editor-in-chief in several peer review journals, chairman and technical program committee in several international conferences. His current research interests include microcontroller, electronics, biomedical signal processing, machine learning, rehabilitation engineering, and surface electromyography (sEMG)-based physical human robot interactions. He can be contacted at email: triwiyanto123@gmail.com.



**Tri Bowo Indarto**    born in Klaten on November 18, 1958. He specializes in nuclear engineering and electrical engineering. He completed his undergraduate in nuclear engineering and his master's degree in electrical engineering at Institut Teknologi Sepuluh Nopember Surabaya, Indonesia. His academic publications cover a range of topics, including the design of microcontroller-based systems, the development of software for diagnostic tools in hemodialysis machines, and the invention of an automatic hand dryer with UV sterilization capabilities. He can be contacted at email: tb\_ind@yahoo.co.id.